ROBUST ADAPTIVE BEAMFORMING: EXPERIMENTAL RESULTS

A.B. Gershman *E. Németh* *J.F. Böhme*

Signal Theory Group
Department of Electrical Engineering
Ruhr University, D-44780 Bochum, Germany
gsh@sth.ruhr-uni-bochum.de

ABSTRACT

The performances of adaptive array algorithms are known to degrade in scenarios with moving interfering sources. Recently, several robust approaches have been proposed to overcome this problem. Below, we compare conventional and robust algorithms using shallow sea sonar data with moving co-channel interference originated from shipping noise. This data set was recorded by a towed horizontal Uniform Linear Array (ULA) of 15 hydrophones. Our real data processing results demonstrate drastic performance improvements that can be achieved using robust algorithms relative to conventional adaptive beamforming techniques.

1. INTRODUCTION

Adaptive array algorithms [1]-[4] are known to degrade in scenarios with moving co-channel interference [5]-[7]. As a rule, this degradation occurs due to a rapid motion of interfering sources or because of array motion (e.g., towed arrays, arrays with moving platforms, etc.). Such limitation of adaptive algorithms is especially strong for large arrays because of relatively sharp notches of adapted pattern [5]. Recently, several robust algorithms have been proposed to overcome this problem either via artificial widening of adaptive pattern nulls [5], [6], or via adaptive allocation of beamformer degrees of freedom [7]. Simulation results in [5]-[7] have shown dramatic performance improvements achieved relative to conventional (non-robust) adaptive array techniques.

Below, we compare several conventional and robust adaptive beamforming algorithms [5] using experimental Baltic Sea data set. This data set was recorded by a towed horizontal ULA of 15 hydrophones in the presence of moving passive interfering sources originating from shipping noise of several moving surface ships.

2. ARRAY DATA MODEL WITH MOVING INTERFERENCES

Assume a ULA of n omnidirectional sensors. Let q ($q < n$) narrowband uncorrelated interfering sources impinge on the array from the unknown directions $\{\theta_1(t), \theta_2(t), \ldots, \theta_q(t)\}$. Then, the output vector of the array at the time t can be expressed as

$$\boldsymbol{y}(t) = \boldsymbol{A}(t)\boldsymbol{x}(t) + \boldsymbol{n}(t) \tag{1}$$

where the $n \times q$ matrix

$$\boldsymbol{A}(t) = [\boldsymbol{a}(\theta_1(t)), \boldsymbol{a}(\theta_2(t)), \ldots, \boldsymbol{a}(\theta_q(t))] \tag{2}$$

is composed of the time-varying interference direction vectors $\boldsymbol{a}(\theta_1(t))$, $\boldsymbol{a}(\theta_2(t)), \ldots, \boldsymbol{a}(\theta_q(t))$. Here $\boldsymbol{a}(\theta)$ is the $n \times 1$ direction vector corresponding to the angle θ,

$$\boldsymbol{x}(t) = (x_1(t), x_2(t), \ldots, x_q(t))^T$$

is the $q \times 1$ vector of random interference waveforms, and $(\cdot)^T$ denotes transpose. The $n \times 1$ vector $\boldsymbol{n}(t)$ contains random sensor noise, and it is assumed for the sake of simplicity that the observations (1) are performed in the absence of signal[1].

Assuming that the noise is statistically independent between the array sensors with the variance σ^2, we can express the $n \times n$ interference-plus-noise covariance matrix as

$$\boldsymbol{R}(t) = \boldsymbol{A}(t)\boldsymbol{R}_{\boldsymbol{x}}\boldsymbol{A}(t)^H + \sigma^2\boldsymbol{I} \tag{3}$$

where

$$\boldsymbol{R}_{\boldsymbol{x}} = \mathrm{E}\{\boldsymbol{x}(t)\boldsymbol{x}^H(t)\}$$

is the $q \times q$ covariance matrix of interference waveforms, $\boldsymbol{I}$ is the identity matrix, and $(\cdot)^H$ denotes Hermitian transpose.

3. CONVENTIONAL TECHNIQUES

The complex adaptive beamformer output with the weight vector $\boldsymbol{w}$ at the time t can be expressed as

$$z(t) = \boldsymbol{w}(t)^H\boldsymbol{y}(t) \tag{4}$$

If the interference-plus-noise covariance matrix $\boldsymbol{R}(t)$ is known, the optimum weight vector of the adaptive array maximizing the Signal-to-Interference-plus-Noise Ratio (SINR) is given by [1], [2]

$$\boldsymbol{w}_{\mathrm{opt}}(t) = \alpha(t)\,\boldsymbol{R}(t)^{-1}\boldsymbol{a}_S \tag{5}$$

This work was supported in parts by Grant Bo 568/22-1 of DFG (Germany) and Grant INTAS-93-642-Ext of INTAS (Belgium).

[1] If the observations contain the signal component, the techniques considered do not need any additional modification except for involving of main-lobe constraints to prevent performance degradation due to signal positioning errors [2], [3].

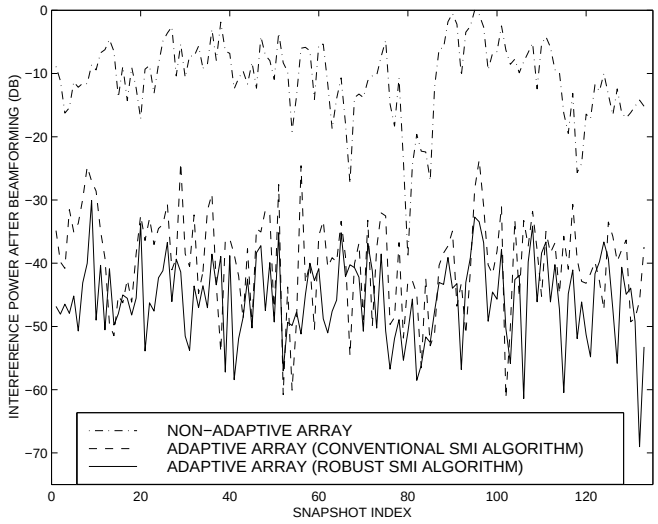

Figure 1: Array outputs (19) vs. the snapshot index t. Conventional beamformer is compared to the conventional and robust ($p = 1$) SMI algorithms with $N = 16$.

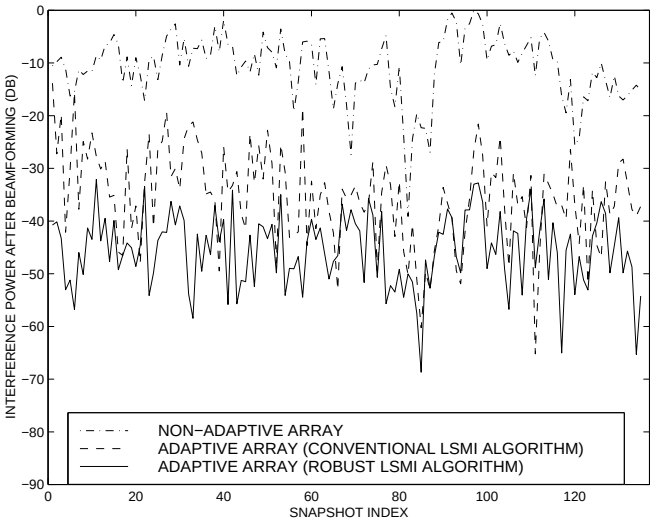

Figure 2: Array outputs (19) vs. the snapshot index t. Conventional beamformer is compared to the conventional and robust ($p = 1$) LSMI algorithms with $N = 14$.

where $\boldsymbol{a}_S$ is the signal direction vector, and $\alpha(t)$ is a norming constant [2], which does not affect the output SINR

$$\mathrm{SINR}(t) = \frac{\sigma_S^2 \, |\boldsymbol{w}(t)^H \boldsymbol{a}_S|^2}{\boldsymbol{w}(t)^H \boldsymbol{R}(t) \boldsymbol{w}(t)} \tag{6}$$

of the beamformer (4).

The Sample Matrix Inversion (SMI) and Loaded Sample Matrix Inversion (LSMI) adaptive array algorithms both approximate the unknown matrix $\boldsymbol{R}(t)$ in (5) using a sliding window estimate. In the SMI algorithm, this estimate is given by

$$\hat{\boldsymbol{R}}(t) = \frac{1}{N} \boldsymbol{Y}(t-k) \boldsymbol{Y}^H(t-k) \tag{7}$$

where

$$\boldsymbol{Y}(t-k) = [\boldsymbol{y}(t-k), \ldots, \boldsymbol{y}(t-k+N-1)] \tag{8}$$

is the $n \times N$ sliding window data matrix, N is the window length, and k defines the window shift relative to the beamforming snapshot $\boldsymbol{y}(t)$ (see (4)). The optimal value of the parameter k depends on specific application of the algorithm [5].

The LSMI algorithm represents a variant of the SMI method that enables the application to very short sliding windows [4]. It uses a small positive diagonal load of the sample covariance matrix to warrant the sample covariance matrix invertibility, i.e.,

$$\hat{\boldsymbol{R}}_{\mathrm{DL}}(t) = \gamma \boldsymbol{I} + \hat{\boldsymbol{R}}(t) \tag{9}$$

The choice of γ is discussed in [4].

Another class of popular methods exploits directly the subspace properties of data snapshots and approximates the matrix $\boldsymbol{R}^{-1}(t)$ in (5) by means of orthogonal projector onto the subspace which is orthogonal to the interference-subspace [5], [8]. For example, the Hung-Turner (HT) algorithm [8] approximates the optimal weight vector (5) as

$$\boldsymbol{w}_{\mathrm{HT}}(t) = \alpha(t) \, \boldsymbol{P}^{\perp}_{\boldsymbol{Y}(t-k)} \boldsymbol{a}_S \tag{10}$$

where

$$\boldsymbol{P}_{\boldsymbol{C}} = \boldsymbol{C}(\boldsymbol{C}^H \boldsymbol{C})^{-1} \boldsymbol{C}^H, \quad \boldsymbol{P}^{\perp}_{\boldsymbol{C}} = \boldsymbol{I} - \boldsymbol{P}_{\boldsymbol{C}} \tag{11}$$

are the orthogonal projectors on the column space of arbitrary $n \times m$ ($n > m$) full rank matrix $\boldsymbol{C}$, and onto its orthogonal complement, respectively.

The optimal value of N can be derived analytically for the HT algorithm (10) under rather mild assumptions [9].

4. ROBUST TECHNIQUES

In the presence of rapidly moving (non-stationary) interferences, the sliding window estimate (7) and (8) may we very poor since it is based on the stationarity assumption. In other words, if the co-channel interference is highly non-stationary at the window length then interfering sources may move away from the sharp notches of the adapted pattern, and this may lead to a strong degradation of the output SINR [5]. An efficient remedy for adaptive array performance in such situations is based upon artificial broadening of the null width toward the directions of interfering sources [6]. This broadening can be achieved by imposing of the so-called *data-dependent derivative constraints* (see [5] for details).

With these constraints up to the pth order, the robust SMI algorithm [5] is given by

$$\boldsymbol{w}_{\mathrm{rob}}(t) = \alpha(t) \, \tilde{\boldsymbol{R}}^{-1}(t) \boldsymbol{a}_S \tag{12}$$

where

$$\tilde{\boldsymbol{R}}(t) = \hat{\boldsymbol{R}}(t) + \sum_{i=1}^{p} \zeta_p \, \boldsymbol{B}^p \hat{\boldsymbol{R}}(t) \boldsymbol{B}^p \tag{13}$$

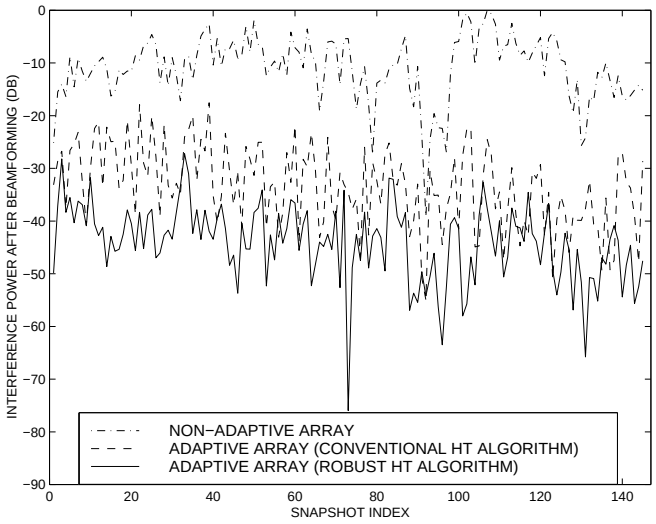

Figure 3: Array outputs (19) vs. the snapshot index t. Conventional beamformer is compared to the conventional and robust ($p = 1$) HT algorithms with $N = 4$.

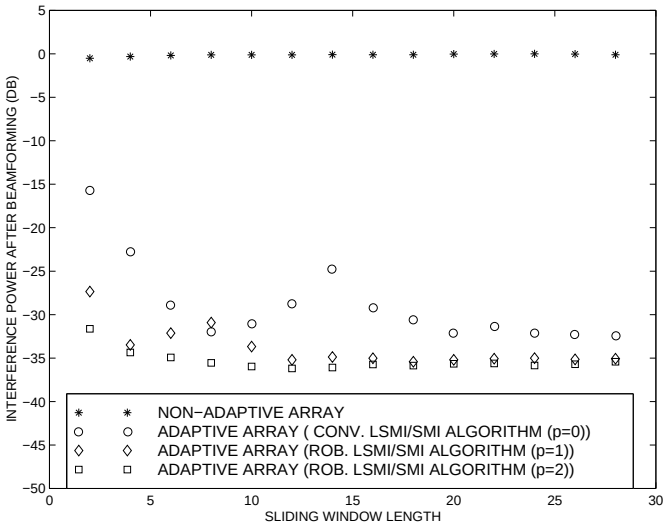

Figure 4: Array outputs (19) vs. N. Conventional beamformer is compared to the conventional and robust ($p = 1$) LSMI/SMI algorithms. The outputs (19) were additionally averaged over the snapshot index t. For $N < n$, LSMI algorithm was used. For $N \geq n$, SMI algorithm was used.

is the estimate of the covariance matrix including the data-dependent constraints, and $\boldsymbol{B}$ is the $n \times n$ diagonal matrix of sensor coordinates [5]. Usually, even the first order of constraints ($p = 1$) suffices for an improved robustness, although higher orders are shown to provide additional improvements [6]. Under very mild conditions, the optimal values of constraint weights ζ_i ($i = 1, \ldots, p$) do not depend on source parameters (i.e., depend on the array geometry only). This fact is shown in [5] for $p = 1$ and can be proven for $p > 1$ as well.

The robust LSMI algorithm represents a straightforward modification of (12):

$$\boldsymbol{w}_{\rm rob}(t) = \alpha(t)\, \tilde{\boldsymbol{R}}^{-1}_{\rm DL}(t)\boldsymbol{a}_S \qquad (14)$$

where

$$\tilde{\boldsymbol{R}}_{\rm DL}(t) = \gamma \boldsymbol{I} + \tilde{\boldsymbol{R}}(t) \qquad (15)$$

The robust modification of the HT algorithm is given by [6]

$$\boldsymbol{w}_{\rm rob}(t) = \alpha(t)\, \boldsymbol{P}^{\perp}_{\boldsymbol{Q}_{(t-k)}}\boldsymbol{a}_S \qquad (16)$$

where

$$\boldsymbol{Q}(t) = [\boldsymbol{Y}(t), \boldsymbol{B}\boldsymbol{Y}(t), \ldots, \boldsymbol{B}^p\boldsymbol{Y}(t)] \qquad (17)$$

In contrast to (13), no weights ζ_i ($i = 1, \ldots, p$) are necessary in (16).

5. DESCRIPTION OF SONAR DATA

The experimental site was located in the Bornholm Deep, east of Bornholm island in the Baltic Sea. The experiments were conducted by Atlas Elektronik (Bremen), in October 1983. A towed horizontal hydrophone ULA of 15 sensors was used. The array parameters were as follows: interelement spacing $d = 2.56$ m, sampling frequency $f_s = 1024$ Hz after low pass-filtering with cut-off 256 Hz. The "narrowband" snapshots were formed from this broadband data after DFT at the single frequency $f = 196.25$ Hz, and the interval between neighboring snapshots was chosen to be 4 seconds. A record of 10 minutes duration (i.e., with 150 successive snapshots) was used. The co-channel interference was originated from a shipping noise.

Much more details on this experiment and experimental data parameters may be found in [10], [11]. In particular, from the analysis of covariance matrix eigenvalues in [10] it follows that there were four moving and non-moving ships (co-channel interferences). The interference power was $10 \div 20$ dB higher than that of noise in a single array sensor. The sea depth at the experimental site was about $60 \div 65$ m [10].

6. REAL DATA PROCESSING

The idea of experimental data processing was to assume some (nominal) signal direction $\boldsymbol{a}_S$ and to impose a mainlobe constraint [2], [3]

$$\boldsymbol{w}^H\boldsymbol{a}_S = 1 \qquad (18)$$

for each algorithm tested. Then, to compare the performance of conventional and robust algorithms, it is necessary to compare the real (squared) outputs

$$|z(t)|^2 = |\boldsymbol{w}(t)^H\boldsymbol{y}(t)|^2 \qquad (19)$$

for each algorithm. The output (19) shows the remaining parts of the co-channel interference and noise power after adaptive beamforming/rejection and, therefore, directly reflects the performance. In other words, the lower the output (19), the better the co-channel interference is rejected. In Figs.1-3, the output (19) of non-adaptive (conventional) beamformer

$$\boldsymbol{w}_{\rm conv} = \frac{\boldsymbol{a}_S}{\boldsymbol{a}_S^H\boldsymbol{a}_S} \qquad (20)$$

is compared with that of the conventional and robust SMI, LSMI, and HT algorithms, respectively. Note that the condition (18) is satisfied for (20) as well. In each figure, the maximum of the output (19) for conventional beamformer was normed to 0 dB. The nominal signal direction assumed was $\theta_S = -20°$. Throughout real data processing, we assumed that each sliding window (8) was followed by the beamforming snapshot $\boldsymbol{y}(t)$, i.e., the beamforming snapshot was just the next one after the window. This sampling scheme corresponds to the particular choice $k = N$ in (8). In Figs. 1-3, the window length N of conventional/robust SMI, LSMI, and HT algorithms was 16, 14, and 4 snapshots, respectively.

Figs. 4 and 5 demonstrate the performances of different algorithms versus the sliding window length. The robust algorithms with $p = 1, 2$ have been tested. In these figures, the outputs (19) were additionally averaged over the snapshot index t.

7. DISCUSSION

From Figs. 1-5, it follows that the performance improvements due to the robust algorithms are very significant. Figs 4 and 5 enable to find an appropriate window length for different methods in sense of performance-complexity tradeoff. The most pronouncing improvements have been achieved for the HT algorithm with short window lengths. However, its window length should be carefully adjusted in practice to avoid the unnecessary degradation of performance [10]. Even for the optimal window length for each algorithm, there are visible improvements due to the robust algorithms (more than $3 \div 5$ dB) in Figs. 4 and 5.

From Figs. 4 and 5, it also follows that the second-order data-dependent constraints can further improve the performance relative to the first-order constraints.

8. CONCLUSIONS

We compared conventional and robust adaptive array algorithms using shallow sea sonar data with moving co-channel interference originated from shipping noise. Our results demonstrate drastic performance improvements that can be achieved using robust algorithms relative to conventional adaptive beamforming techniques. Other applications of our robust algorithms are radar and wireless communications.

9. REFERENCES:

[1] I.S. Reed, J.D. Mallett, and L.E. Brennan, "Rapid convergence rate in adaptive arrays," *IEEE Transactions on Aerospace and Electron. Systems*, vol. AES-10, pp. 853-862, November 1974.

[2] R.A. Monzingo and T.W. Miller, *Introduction to Adaptive Arrays*, New York: Wiley, 1980.

[3] J.E. Hudson, *Adaptive Array Principles*, IEE: Peter Peregrinus, Stevenage, UK, and New York, 1981.

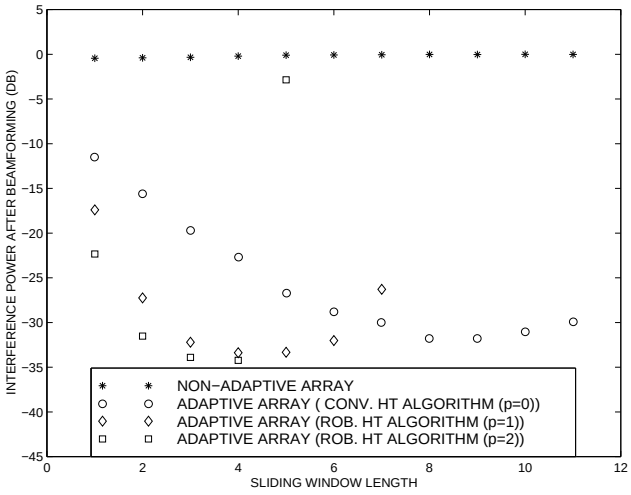

Figure 5: Array outputs (19) vs. N. Conventional beamformer is compared to the conventional and robust ($p = 1$) HT algorithms. The outputs (19) were additionally averaged over the snapshot index t.

[4] B.D. Carlson, "Covariance matrix estimation errors and diagonal loading in adaptive arrays," *IEEE Transactions on Aerospace Electron. Systems*, vol. AES-24, pp. 397-401, July 1988.

[5] A.B. Gershman, U. Nickel, and J.F. Böhme, "Adaptive beamforming algorithms with robustness against jammer motion," *IEEE Transactions on Signal Processing*, vol. SP-45, pp. 1878-1885, July 1997.

[6] A.B. Gershman, G.V. Serebryakov, and J. F.Böhme, "Constrained Hung-Turner adaptive beamforming algorithm with additional robustness to wideband and moving jammers,"*IEEE Transactions on Antennas and Propagation*, vol. AP-44, pp. 361-367, March 1996.

[7] J. Riba, J. Goldberg, G. Vazquez, "Robust beamforming for interference rejection in mobile communications," *IEEE Transactions on Signal Processing*, vol. SP-45, pp. 271-275, January 1997.

[8] E.K. Hung, and R.M. Turner, "A fast beamforming algorithm for large arrays," *IEEE Transactions on Aerospace and Electron. Systems*, vol. AES-19, pp. 598-607, July 1983.

[9] C.H. Gierull, "Performance analysis of fast projections of the Hung-Turner type for adaptive beamforming," *Signal Processing*, vol. 50, 1996, pp. 17-28, April 1996.

[10] C.F. Mecklenbräuker, A.B. Gershman, and J.F. Böhme, "Broadband ML-approach to environmental parameter estimation in shallow ocean at low SNR," submitted to *IEEE Journal on Oceanic Engineering*, 1997.

[11] C.F. Mecklenbräuker, A.B. Gershman, and J.F. Böhme, "ML-estimation of environmental parameters in shallow ocean using unknown broadband sources," invited paper in *Proceedings Intern. Conf. Neural Networks and Signal Processing, ICNNSP'95*, pp. 1091-1094, Nanjing, December 1995.